Total Least Squares in Robot Calibration

John Hollerbach and Ali Nahvi

Depts. Computer Science and Mechanical Engineering
University of Utah, Salt Lake City, UT 84112
jmh@cs.utah.edu

Abstract

The role of input noise is seldom considered in robot calibration. The methodology of total least squares may be applied to handle both input and output noise in robot calibration. Experimentally, we apply this method towards joint torque sensor calibration, and towards kinematic calibration of a redundant parallel-drive spherical joint in a variant called the implicit loop method.

1. Introduction

Previous work in robot calibration has almost exclusively employed Ordinary Least Squares (OLS), applied in nonlinear cases to the linearized equations iteratively. The premise for OLS is that the output or dependent variable in an explicit equation is the only source of measurement error. Yet errors in the input or independent variables are often significant, and the use of OLS in the presence of input error or noise is known to lead to bias errors in the estimates [10].

The issue of input noise is known in the statistics literature as the errors-in-variables problem [3]. Figure 1A illustrates the simple case of fitting a straight line $y = ax$. OLS assumes that the only error is in the ouput variable y; the input variable x is presumed known exactly. Hence the squared vertical distances $\Delta y^i = y^i - y_c^i$ from P measured data points (x^i, y^i) to the corresponding computed points (x_c^i, y_c^i) on the fitted line $y_c^i = ax_c^i$ should be minimized (Figure 1A(a)):

$$\min_{a, x_c^i, y_c^i} \sum_{i=1}^{P} (\Delta y^i)^2 \quad \text{subject to } y_c^i = ax_c^i \tag{1}$$

Besides the slope a, OLS also determines the computed "correct" point locations (x_c^i, y_c^i) on the fitted line for each point i, where $x_c^i = x^i$. The other coordinate y_c^i is eliminated from (1) by substituting the explicit constraint equation $y_c^i = ax_c^i$:

$$\min_{a} \sum_{i=1}^{P} (y^i - ax^i)^2 \tag{2}$$

This is the normal least squares formulation, whose origin from (1) is instructive for subsequent developments.

Suppose now that there is only input noise, i.e., in x^i. Then $y_c^i = y^i$ and we should minimize the horizontal fitting error $\Delta x^i = x^i - x_c^i$ (Figure 1A(b)):

$$\min_{a, x_c^i, y_c^i} \sum_{i=1}^{P} (\Delta x^i)^2 \quad \text{subject to } y_c^i = ax_c^i \tag{3}$$

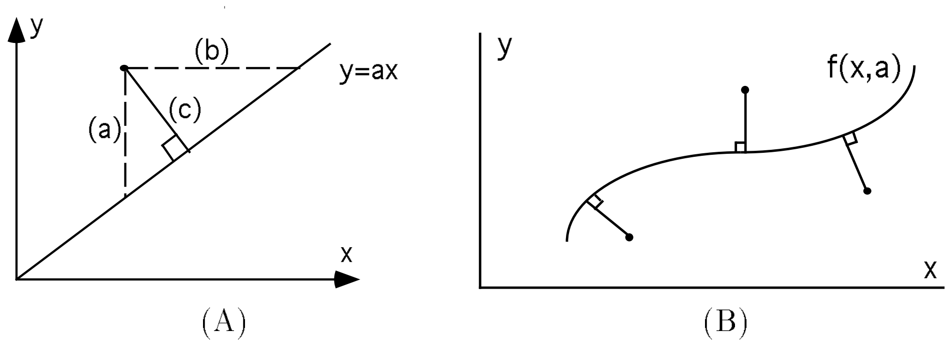

Figure 1. (A) Fitting a straight line in case of (a) output noise only, (b) input noise only, and (c) equal input and output noise. (B) Nonlinear orthogonal distance regression.

The unknown line coordinate x_c^i is again eliminated by incorporating the constraint equation into the objective function:

$$\min_a \sum_{i=1}^{P} (x^i - y^i/a)^2 \tag{4}$$

This process has simply exchanged the role of dependent and independent variable.

Next suppose that there are equal errors in the x and y variables. Then we should fit the orthogonal distance from the data to the line (Figure 1A(c)):

$$\min_{a,x_c^i,y_c^i} \sum_{i=1}^{P} (\Delta x^i)^2 + (\Delta y^i)^2 \quad \text{subject to } y_c^i = a x_c^i \tag{5}$$

The orthogonal distance means that the line from (x^i, y^i) to (x_c^i, y_c^i) should be perpendicular to the fitted line $y_c^i = a x_c^i$. Incorporating orthogonality and the constraint equation yields the objective function:

$$\min_a \sum_{i=1}^{P} \frac{(y_i - a x_i)^2}{1 + a^2} \tag{6}$$

A final embellishment is to suppose that there are unequal uncertainties in the input/output variables, given by the standard deviations σ_x and σ_y. Then the weighted normal distances from points (x_i, y_i) to the line are minimized:

$$\min_{a,x_c^i,y_c^i} \sum_{i=1}^{P} \frac{(\Delta x^i)^2}{\sigma_x^2} + \frac{(\Delta y^i)^2}{\sigma_y^2} \quad \text{subject to } y_c^i = a x_c^i \tag{7}$$

After substitution of the constraint equation, one eventually gets

$$\min_a \chi^2 = \sum_{i=1}^{P} \frac{(y_i - a x_i)^2}{\sigma_y^2 + a^2 \sigma_x^2} \tag{8}$$

which is written as a χ^2 statistic [11], i.e., the least-squares sum has a χ^2 distribution with expected value $E(\chi^2) = P - 1$. The expected value says nothing more than that the experimentally measured standard deviations should be about the same as the *a priori* standard deviations. The number of measurements P is reduced by 1 to

$P-1$ because the squared terms are not independent, as the equivalent of one has been used to determine a. The number $\nu = P-1$ is called the *degrees of freedom* in the statistics literature (unfortunate conflict with robotics terminology), and reflects the excess of measurements over fitted parameters.

The solution to the orthogonal distance objective function (8) looks like a nonlinear optimization problem, and has been solved as such in [11]. This procedure is however unnecessary in the linear case, as analytic procedures exist. The solution to the errors-in-variables problem is known as *total least squares* in the numerical analysis literature [12] and as *orthogonal distance regression* in the statistics community [2]. The analytic solution in the total least squares approach uses singular value decomposition.

Orthogonal distance regression has been known since last century, and has been often rediscovered under various guises. In robotics and vision, one common application of orthogonal distance regression is to fit a plane to a set of measured 3D points; all 3 components of measured position have noise (e.g., [5]). The ties to the literature in the numerical analysis and statistics communities have unfortunately seldom been made. On the other hand, the major developments in these communities on handling input noise have been recent, especially for nonlinear optimization.

Recently, Wampler et al. [13] have introduced an approach towards nonlinear orthogonal distance regression for the problem of kinematic calibration, termed the *Implicit Loop Method* (ILM). Key features of this method that distinguish it from previous approaches are the use of an implicit constraint equation, based on a notion that kinematic calbration approaches can nearly all be viewed as closed-loop approaches with the sensor as a joint [7], and the use of *a priori* parameter estimates. In this paper, we apply this method to two different calibration problems: (1) the calibration of joint torque sensors, and (2) the calibration of a parallel-drive shoulder joint.

2. Implicit Loop Method

Consider fitting a scalar function $y = f(x, a)$ by adjusting parameters a. In case of equivalent error in x and y measurements, we should again minimize the Euclidean distances from the measurements to the fitted curve f (Figure 1B):

$$\min_{a, x_c^i, y_c^i} \sum_{i=1}^{P} (\Delta x^i)^2 + (\Delta y^i)^2 \quad \text{subject to } y_c^i = f(x_c^i, a) \tag{9}$$

This nonlinear constrained optimization problem is solved by linearization and iteration [2], but the solution is presented in a more general context next.

Implicit constraint equations can arise in kinematic calibration of mulitple-loop mechanisms. Even for serial chains, Hollerbach and Wampler [7] take the viewpoint that nearly all calibration methods can be cast as closed-loop methods. Consider an implicit loop-closure constraint equation

$$\mathbf{0} = \mathbf{f}(\mathbf{x^i}, \mathbf{p}) \tag{10}$$

All measurements, whether endpoint sensing or joint angles, are lumped into a measurement vector $\mathbf{x}^i$. The vector $\mathbf{p}$ contains all unknown parameters. Let $\mathbf{x}$ represent the stacked vector for all poses i and redefine $\mathbf{f}$ as well.

We separate the vector $\mathbf{x} = \mathbf{x}_0 + \mathbf{x}_e$, where $\mathbf{x}_0$ is the measurement and $\mathbf{x}_e$ is the measurement error. Also set $\mathbf{p} = \mathbf{p}_0 + \mathbf{p}_e$, where $\mathbf{p}_0$ are a priori estimates for the parameters. Incorporate $\mathbf{x}_0$ and $\mathbf{p}_0$ as constants into the loop closure equation (10), which is then a function $\mathbf{f}'(\mathbf{x}_e, \mathbf{p}_e) = \mathbf{0}$. Then minimize the optimization function

$$\min_{\mathbf{x}_e, \mathbf{p}_e} \mathbf{x}_e^T \mathbf{V}_x^{-1} \mathbf{x}_e + \mathbf{p}_e^T \mathbf{V}_p^{-1} \mathbf{p}_e \tag{11}$$

subject to $\mathbf{f}'(\mathbf{x}_e, \mathbf{p}_e) = \mathbf{0}$, where $E(\mathbf{x}_e \mathbf{x}_e^T) = \mathbf{V}_x$ and $E(\mathbf{p}_e \mathbf{p}_e^T) = \mathbf{V}_p$ are covariance estimates. Again, this function is a χ^2 statistic. Note that the objective function biases the solution to the a priori values.

Because of the implicit constraint equation, direct substitution into the objective function to eliminate some unknowns is not possible. Instead, the equations are linearized and variable elimination is achieved through QR decomposition [13]. Let the scaled variables $\mathbf{y}$ and $\mathbf{q}$ be defined via $\mathbf{x}_e = \mathbf{V}_x^{1/2}\mathbf{y}$ and $\mathbf{p}_e = \mathbf{V}_p^{1/2}\mathbf{q}$, where the superscript 1/2 means the symmetric square root. Iterate from an initial guess $\mathbf{y} = \mathbf{0}$ and $\mathbf{q} = \mathbf{0}$ to find corrections $\Delta\mathbf{y}$ and $\Delta\mathbf{q}$ to minimize

$$\chi^2 = (\mathbf{y} + \Delta\mathbf{y})^T(\mathbf{y} + \Delta\mathbf{y}) + (\mathbf{q} + \Delta\mathbf{q})^T(\mathbf{q} + \Delta\mathbf{q}) \tag{12}$$

subject to the linearized constraints

$$-\mathbf{f}'(\mathbf{y}, \mathbf{q}) = \frac{\partial \mathbf{f}'}{\partial \mathbf{y}}(\mathbf{y}, \mathbf{q})\Delta\mathbf{y} + \frac{\partial \mathbf{f}'}{\partial \mathbf{q}}(\mathbf{y}, \mathbf{q})\Delta\mathbf{q} \equiv \mathbf{J}_y \Delta\mathbf{y} + \mathbf{J}_q \Delta\mathbf{q} \tag{13}$$

Compute the QR-decomposition $\mathbf{Q}\tilde{\mathbf{R}} = \mathbf{J}_y^T$ and define

$$\mathbf{D} = \tilde{\mathbf{R}}^{-T}\mathbf{J}_y, \quad \mathbf{E} = \mathbf{Q}^T\mathbf{y} - \tilde{\mathbf{R}}^{-T}\mathbf{f}(\mathbf{y}, \mathbf{q}) \tag{14}$$

The variables $\Delta\mathbf{y}$ are eliminated and the step in $\mathbf{q}$ found from:

$$\begin{bmatrix} \mathbf{D} \\ \mathbf{I} \end{bmatrix} \Delta\mathbf{q} = \begin{bmatrix} \mathbf{E} \\ -\mathbf{q} \end{bmatrix} \tag{15}$$

and the updated error estimates are

$$\mathbf{y} + \Delta\mathbf{y} = \mathbf{Q}(\mathbf{E} - \mathbf{D}\mathbf{q}) \tag{16}$$

Later we will use the definition $\hat{\mathbf{D}} = [\mathbf{D}^T\mathbf{I}]^T$, to examine the effect of a priori estimates on singular values.

3. Torque Sensor Calibration

Ma et al. [8] developed an autonomous joint torque sensor calibration, which utilizes combinations of single-joint rotations and an arm's own gravity load. A key feature of the approach is that nothing is assumed known about the arm's inertial parameters or of the location of a reference load in the grasp. The method has been applied to the Sarcos Dextrous Arm Master and Slave (Figure 2). The method determines not only joint torque sensor gains and offsets, but also those of the joint angle sensors.

Individual joint rotation results in a sinusoidal torque versus angle relation:

$$\tau^i = A\sin(k\psi^i + \delta) + \gamma = f(\mathbf{p}, \psi^i) \tag{17}$$

with unknown parameters $\mathbf{p} = (A, k, \delta, \gamma)$ given P input/output measurements ψ^i, τ^i. From the fitted parameters one may extract torque sensor and joint angle sensor gains and offsets; the details may be found in [8]. The ILM was applied,

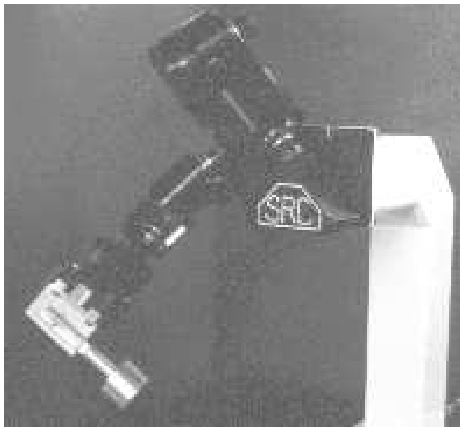

Figure 2. Automatic torque sensor calibration for the Sarcos Dextrous Arm Slave.

without however utilizing a priori parameter values. The weighted objective function is:

$$\min_{\mathbf{p},\psi_c^i,\tau_c^i} \sum_{i=1}^{P} \frac{(\Delta\psi^i)^2}{\sigma_\psi^2} + \frac{(\Delta\tau^i)^2}{\sigma_\tau^2} \quad \text{subject to } \tau_c^i = f(\mathbf{p}, \psi_c^i) \tag{18}$$

where $\Delta\psi^i = \psi^i - \psi_c^i$ and $\Delta\tau^i = \tau^i - \tau_c^i$ and the subscript c again stands for computed. The uncertains in the input/output measurements are σ_ψ and σ_τ. Again the constraint equation is substituted to eliminate the τ_c^i unknowns.

Results are presented in Table 1 for joint 1 of the Sarcos Master in the case of equal weighting for OLS versus ILM. The parameters are fairly close, because of low noise in the data. At present there is no independent method for ascertaining the accuracy of one parameter set over the other, except simulation studies.

Method	**A**	**k**	δ	γ
OLS	372.96	0.00076419	1.8730	2014.6
ILM	373.08	0.00076390	1.8735	2014.7

Table 1. Sinusoidal parameters for OLS versus ILM.

4. Kinematic Calibration of Redundant Parallel-Drive Robot

The mechanism is a 3-DOF platform type closed-chain mechanism with its output link constrained to undergo spherical motions (Figure 3A) [4]. Previously we performed ordinary least squares kinematic calibration [9]; the present section is a reanalysis of the data via the implicit loop method.

The kinematic model is shown in Figure 3B. $\mathbf{A}_i$, $i = 1, \ldots, 4$, represents a spherical joint at the stationary side of each actuator. d_i, $i = 1, \ldots, 4$, is the input of the mechanism and represents a pair of actuator and displacement sensor. $\mathbf{B}_1$ and $\mathbf{B}_2$ are universal joints and lie in the intersection of the centerlines of each two adjacent actuators. Plane $\mathbf{B}_1\mathbf{B}_2\mathbf{O}$ defines the end plate which should be placed into the desired orientation. k_1 and k_2 are imaginary links which are used in calibration loops.

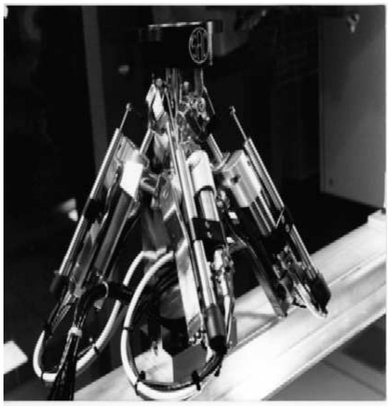

(A)

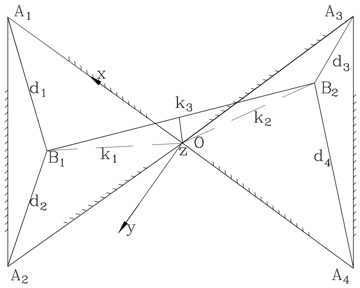

(B)

Figure 3. (A) 3-DOF redundant shoulder joint. (B) Kinematic model viewed from above.

4.1. Calibration Procedure

Since not all angles are sensed in this mechanism, the simplest way to formulate calibration equations is to use distance equations. We use measurement redundancy to establish our objective function which is to be minimized. Assume we move the mechanism into P different poses. Define the vector function $\mathbf{f}$ with components:

$$f(k) = (\mathbf{B}_1(k) - \mathbf{B}_2(k))^2 - k_3^2 + x(k) = 0 \tag{19}$$

where $k = 1, ..., P$ represents the pose number. $\mathbf{B}_1(k)$ and $\mathbf{B}_2(k)$ are the position vectors of the end plate universal joints in pose k. $x(k)$ is an error term and makes $f(k)$ equal to zero. We find $\mathbf{B}_1(k)$ by the intersection of the following three spheres:
Sphere 1: centered at $\mathbf{O}$ with radius k_1,
Sphere 2: centered at $\mathbf{A}_1$ with radius $d_1(k)$,
Sphere 3: centered at $\mathbf{A}_2$ with radius $d_2(k)$.

Then we find $\mathbf{B}_2(k)$ by the intersection of the following three spheres:
Sphere 1: centered at $\mathbf{O}$ with radius k_2,
Sphere 2: centered at $\mathbf{A}_3$ with radius $d_3(k)$,
Sphere 3: centered at $\mathbf{A}_4$ with radius $d_4(k)$.

Length $d_i(k)$ which is measured by LVDT i in pose k is obtained as follows:

$$d_i(k) = s_i * v_i(k) + d_{0i} \; (i = 1, ..., 4, k = 1, ..., P) \tag{20}$$

where s_i, $v_i(k)$, and d_{0i} represent the gain, output voltage, and offset of LVDT i respectively. It is worth mentioning that each time LVDTs are disassembled and then reassembled, d_{0i} may change considerably (a few millimeters) and the closed-loop calibration is a promising approach for finding new offsets.

The objective function and solution procedure were outlined in Section 2.

4.2. Simulation Results

The selection of the parameters to be calibrated is an important issue. While we would ideally identify all the kinematic parameters, we should first evaluate the limits of the approach by considering measurement errors due to resolution, nonlinearity, noise of sensors, and the numerical error of the method used. We may then decide which parameters should be assumed known and which should be identified.

Param.	True value	Initial guess	Result
d_{01}	90.0	80.0	89.9
d_{02}	90.0	95.0	90.2
d_{03}	90.0	85.0	90.0
d_{04}	85.0	90.0	85.0
s_1	3.659	3.660	3.659
s_2	3.656	3.660	3.659
s_3	3.658	3.660	3.661
s_4	3.660	3.660	3.662

(A)

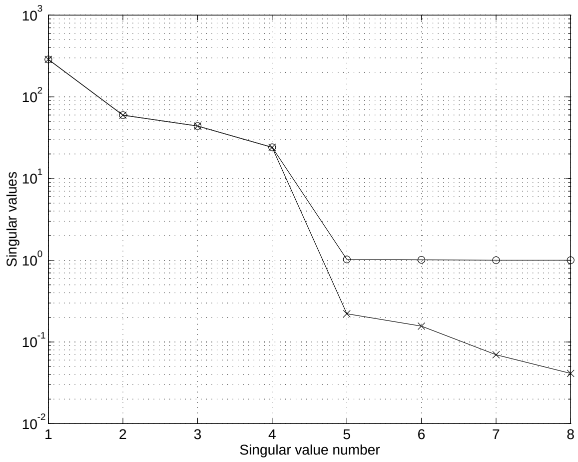

(B)

Figure 4. (A) Simulation results of the shoulder joint calibration. Units for d_{0i}: mm. Units for s_i: mm/v. (B) Singular values of the fitting matrices $\mathbf{D}$ (x) and $\hat{\mathbf{D}}$ (o).

In order to find the accuracy of the sensors, we moved each LVDT off-line using an accurate milling machine and found that the overall accuracy of each sensor is about 40mv (0.15 mm). We treat this error as noise, though it is due to a combination of sensor nonlinearity, noise, and resolution. On the other hand, the mechanical parts of this robot have a manufacturing tolerance better than 0.1mm. Considering the 0.15mm sensor noise, it is not useful to calibrate those kinematic parameters which already have a better accuracy in blue print data than the sensor noise. Thus we should only calibrate the sensor offsets and gains. The parameter vector $\mathbf{p}$ is defined as:

$$\mathbf{p} = [d_{01}\ d_{02}\ d_{03}\ d_{04}\ s_1\ s_2\ s_3\ s_4]^T \tag{21}$$

We added Gaussian noise of 40mv (0.15mm) to the sensor readings derived from simulation. Each pose set contained 50 poses. The standard deviation for sensor offsets was set to 7.0, for sensor gains to 0.005, and for the residual error function to 49.0. Thus the weighting matrices are:

$$\mathbf{V}_p = \mathrm{diag}[\frac{1}{7^2}, \frac{1}{7^2}, \frac{1}{7^2}, \frac{1}{7^2}, \frac{1}{.005^2}, \frac{1}{.005^2}, \frac{1}{.005^2}, \frac{1}{.005^2}] \tag{22}$$

$$\mathbf{V}_x = [\frac{1}{49^2}] \tag{23}$$

Figure 4A shows the results. It is seen that calibration results are close to true values, but we were suspicious about the accuracy of scale factors because the results were somewhat dependent on our initial guess. Figure 4B shows the singular values for the fitting matrices $\mathbf{D}$ and $\hat{\mathbf{D}}$. It is seen that the last four singular values of $\mathbf{D}$ are much smaller than 1, resulting in poor values for the gains. In other words, four singular values of $\hat{\mathbf{D}}$ are almost equal to 1, indicating no reduction in the uncertainty of our initial guess for gains. The χ^2 value is 49.5 which is near the expected value of 50.

Param.	**Initial guess**	**Result**
d_{01}	95.0	96.8
d_{02}	95.0	99.2
d_{03}	95.0	95.9
d_{04}	95.0	101.9
s_1	3.697	3.697
s_2	3.586	3.586
s_3	3.604	3.604
s_4	3.678	3.677

(A)

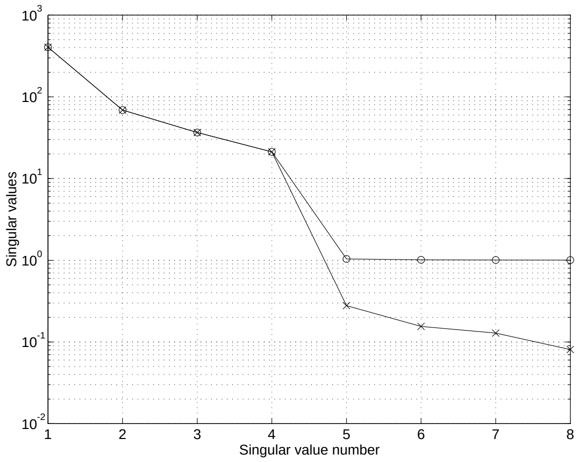

(B)

Figure 5. (A) Experimental results of the shoulder joint calibration. (B) Singular values of the fitting matrices $\mathbf{D}$ (x) and $\hat{\mathbf{D}}$ (o) resulting from experimental data of the shoulder joint.

4.3. Experimental Results

The end plate was moved into different orientations manually and data were acquired simultaneously from four LVDT's through 12-bit A/D converters with a sampling frequency of 20 Hz. 450 poses were recorded. We wrote an algorithm in MATLAB to select 50 poses out of 450 poses to have a good observability index [7]. The weighting matrices were defined as:

$$\mathbf{V}_p = \mathrm{diag}[\frac{1}{6^2}, \frac{1}{6^2}, \frac{1}{6^2}, \frac{1}{6^2}, \frac{1}{.005^2}, \frac{1}{.005^2}, \frac{1}{.005^2}, \frac{1}{.005^2}] \quad (24)$$

$$\mathbf{V}_x = [\frac{1}{36^2}] \quad (25)$$

Figure 5A shows the results. Again, we suspected about the accuracy of scale factors because the results were somewhat dependent on our initial guess. Figure 5B shows the singular values for the fitting matrices $\mathbf{D}$ and $\hat{\mathbf{D}}$. The results are very similar to simulation, indicating no improvement in the uncertainty of our initial guess for gains. We expect a χ^2 value of 50 with a standard deviation of 10. The χ^2 value obtained from the fit is 20.1 which falls within 3σ of its expected value.

5. Conclusions

Input noise is often significant in robot calibration problems, but the approach of total least squares may be applied to these problems. we have presented the application of one variant of this method, the implicit loop method [13], to two different calibration problems. One is torque sensor calibration, the other kinematic calibration of a rendundant parallel-drive spherical mechanism. Results indicate so far that significant although not large differences in parameter estimates are obtained over those based on OLS.

Acknowledgements. This work was supported by National Science Foundation grant MIP-9420352, and by Natural Sciences and Engineering Research Council of Canada Network of Centers of Excellence Institute for Robotics and Intelligent

Systems (IRIS) grant AMD-5.

References

[1] Bennett, D.J., and Hollerbach, J.M., "Autonomous calibration of single-loop closed kinematic chains formed by manipulators with passive endpoint constraints," *IEEE Trans. Robotics and Automation*, vol. 7, pp. 597-606, 1991.

[2] Boggs, P.T., Byrd, R.H., and Schnabel, R.B., "A stable and efficient algorithm for nonlinear orthogonal distance regression," *SIAM J. Sci. Stat. Comput.*, vol. 8, pp. 1052-1078, 1987.

[3] Fuller, W.A., *Measurement Error Models.* NY: John Wiley & Sons, 1987.

[4] Hayward, V., "Design of a hydraulic robot shoulder mechanism based on a combinatorial mechanism," *Preprints of the Third International Symposium on Experimental Robotics.* Kyoto, Japan:, 1993.

[5] Hollerbach, J.M., and Bennett, D.J., "Automatic kinematic calibration using a motion tracking system," *Robotics Research: the Fourth International Symposium*, edited by R. Bolles and B. Roth. Cambridge, MA: MIT Press, pp. 191-198, 1988.

[6] Hollerbach J.M., and Lokhorst, D.M., "Closed-loop kinematic calibration of the RSI 6-DOF hand controller," *IEEE Trans. Robotics and Automation*, vol. 11, pp. 352-359, 1995.

[7] Hollerbach, J.M., and Wampler, C.W., "The calibration index and taxonomy for robot kinematic calibration methods," *Intl. J. Robotics Research*, in press, 1996.

[8] Ma, D., Hollerbach, J.M., and Xu, Y., "Gravity based autonomous calibration for robot manipulators," *Proc. IEEE Intl. Conf. Robotics and Automation*, 1994.

[9] Nahvi, A., Hollerbach, J.M., and Hayward, V., "Calibration of a parallel robot using multiple kinematic closed loops," *Proc. IEEE Intl. Conf. Robotics and Automation*, pp. 407-412, 1994.

[10] Norton, J.P., *An Introduction to Identification.* London: Academic Press, 1986.

[11] Press, W.H., Teukolsky, S.A., Vetterling, W.T., and Flannery, B.P., *Numerical Recipes in C.* Cambridge, UK: Cambridge Univ. Press, 1992.

[12] Van Huffel, S., and Vandewalle, J., *The Total Least Squares Problem: Computational Aspects and Analysis.* Philadelphia: SIAM, 1991.

[13] Wampler, C.W., Hollerbach, J.M., and Arai, T., "An Implicit Loop Method for kinematic calibration and its application to closed-chain mechanisms," *IEEE Trans. Robotics and Automation*, vol. 11, pp. 710-724, 1995.